Measuring Cell Mechanical Properties Using Microindentation

Julien Husson

Julien Husson

LadHyX, CNRS, Ecole polytechnique, Institut Polytechnique de Paris, Palaiseau, France

julien.husson@ladhyx.polytechnique.fr

i. Chapter title

Measuring cell mechanical properties using microindentation

Running head: Cell microindentation

ii. Summary/Abstract

Quantifying cell mechanical properties is of interest to better understand both physiological and pathological cellular processes. Cell mechanical properties are quantified by a finite set of parameters such as the effective Young's modulus or the effective viscosity. These parameters can be extracted by applying controlled forces to a cell, and by quantifying the resulting deformation of the cell.

Microindentation consists in pressing a cell with a calibrated spring terminated by a rigid tip, and by measuring the resulting indentation of the cell. We have developed a microindentation technique that uses a flexible micropipette as a spring. The micropipette has a microbead at its tip, and this spherical geometry allows using analytical models to extract cell mechanical properties from microindentation experiments. We use another micropipette to hold the cell to be indented, which makes this technique well-suited to study non-adherent cells, but we also describe how to use this technique on adherent cells.

iii. Key Words

Microindentation, cell mechanics, micromanipulations, micropipettes, contact mechanics.

1. Introduction

Mechanical properties of cells regulate their shape and dynamics so they are important in many biological processes, including cell migration, division, immune reaction, and development. Furthermore, many pathologies, including cancer, are associated with altered cell mechanical properties (1). As a result, quantifying cell mechanical properties is of interest to better understand both physiological and pathological cellular processes, and might help opening routes for new diagnostic strategies (2).

Cell mechanical properties are quantified by a finite set of parameters such as the effective Young's modulus of the cell (its elasticity – the higher the Young's modulus, the stiffer the cell), its tension, viscosity or viscoelastic modulus. These parameters relate an applied force to a resulting deformation, where both force and deformations can be time-dependent. The principle to extract these parameters is quite universal and consists in applying a controlled constant force and measuring the resulting deformation, or reversely in prescribing a deformation and in quantifying the force needed to keep this deformation constant.

Microindentation techniques usually use a spring terminated by a rigid tip. This spring is used to apply a known force when pressed against a cell. The applied force is measured by measuring the

deformation (deflection) of the spring and multiplying it by the spring stiffness (in N/m). The cell deformation is quantified through the measurements of how much the probe's tip indents the cell. A gold standard for microindentation is atomic force microscopy (AFM), a technique that is highly resolved in space, force, and time. However, this technique is relatively expensive, and presents a surprisingly major difficulty in its design because the AFM probe is in the optical path. As a result, if one wants to quantify the morphology of the cell being indented using light microscopy, the AFM probe hides precisely what one would like to observe.

We have developed a relatively less expensive alternative to perform microindentation of cells. It uses micropipettes as flexible cantilevers, in an approach that we called profile microindentation, or microindentation for short (Fig. 1)(3, 4). Our technique was built on elegant works by others in other biological contexts (5–7) including the micropipette force sensor by Backholm *et al.* (8), developed decades after the idea of using a hollow micropipette as a flexible cantilever was introduced (9). Flexible micropipettes behave like a linear spring, i.e. with a linear relationship between the amplitude of their bending and the force applied perpendicular to their tip. Micropipettes can have bending stiffness as low as 0.2 nN/µm, fifty times lower than the most flexible AFM tips. This extreme flexibility compensates for a more limited spatial resolution when detecting micropipette bending directly from a camera (as opposed to the great accuracy of laser diodes used in AFM). This leads to force resolution comparable to AFM (few piconewtons in our case). The microindentation technique presented here is that it can readily be coupled with another micropipette that is used to hold a cell, which makes this technique well-suited to study non-adherent cells. However, although this requires to grow cells on a support (dextran beads, see below), it can also be used on adherent cells (3).

To make use of the few analytical models that exist to extract cell mechanical properties from microindentation experiments, we developed ways to place microbeads at the tip of flexible micropipettes, with two alternative techniques. The first technique consists in using an open micropipette to aspirate a microbead at its tip. The interest of this technique is that once a bead has been used against a cell, both beads and cells can be discarded, and a new cell can be indented by a new bead. The second technique consists in melting the tip of a flexible micropipette into a glass microbead (Fig. 2). For simplicity, herein we will call both types of modified micropipettes microindenters, except when distinction between them is needed.

We have applied this technique to quantify viscoelastic properties of endothelial cells (3) and of several types of leukocytes: T lymphocytes (and Jurkat T cells) (4, 10–12), B lymphocytes (10, 13) neutrophils and neutrophil-like PLB cells (10, 14).

2. Materials

Consumable

1. Cells, cultured in an incubator at 37°C under 5% CO_2.
2. P1000 and P200 pipettes with cones.
3. Glass-bottom Petri dishes (35mm Diameter, 23mm Well).
4. For adherent cells: dextran microcarrier beads (average bead size 175 μm).
5. Borosilicate glass capillaries (1 mm OD, 0.78 mm ID). See Note 1.

6. Deionized water for the reservoir and tubing.
7. 70° Ethanol to clean surfaces, tubing and reservoirs.
8. 50 mL Luer lock plastic syringe for reservoir (Fig. 1a).
9. 30 mL Luer lock auxiliary plastic syringe for reservoir (#12 in Fig. 1a).
10. 10 mL Luer lock auxiliary plastic syringe to fill micropipettes.
11. Blunt fill needle to mount on the 10 mL auxiliary syringe (18 G).
12. 4-way stopcock for plugging an auxiliary pipette on the reservoir.
13. Cell buffers. We usually perform experiments in RPMI 1640-GlutaMax-I supplemented with 10% fetal calf serum (FCS), 1% penicillin-streptomycin. The presence of FCS is important to avoid cell-pipette and cell-bottom adhesion. FCS can be replaced with bovine serum albumin for its anti-adhesive effect (see Note 2). We keep buffer stocks at 4°C.
14. Dulbecco's Phosphate Buffer Saline (DPBS).
15. Large Petri dish with thick adhesive rubber used as a micropipette and microindenter storage box to keep them safe from dust and collisions.
16. 15-mL plastic tubes to store cell buffer and DPBS close to the experimental setup.
17. Capillary to fill the back of the micropipettes with water.
18. Kimwipes.

Microscope

19. Inverted microscope equipped with differential interference contrast (DIC). DIC is not necessary but it is a great addition to observe cell morphology (intracellular deformation, fine membrane structures etc.).

20. Air suspension anti-vibration table. See Note 3 on vibrations.
21. Microscope objectives: 100x (Plan Fluor, 1.3 numerical aperture, DIC, oil) for experiments, and eventually lower magnification air objectives (40×, 20×, 10×, and 4×) for micropipette positioning. Experiments could be performed with a lower magnification at the expense of space and force resolution.
22. Matlab software, and the free open-source Micro-Manager software (https://micro-manager.org/)(15).
23. CMOS Camera connected to the microscope controlled using a Matlab code calling the Micro-Manager software.
24. If fluorescence is used, LED fluorescence source and filter cube added to the microscope. We control an LED fluorescent light source through transistor-transistor logic (TTL) *via* the Micro-Manager that is itself controlled by a Matlab code). TTL control is ensured by an Arduino Uno card.
25. Computer

Micromanipulation-related equipment

26. Motorized micromanipulator (#7 in Fig. 1a) mounted on a rigid stand with platform (#8 in Fig. 1a). A second motorized micromanipulator might be needed when using a third pipette, e.g. to flow a molecule of interest (such as an inhibitor) on the cell being indented (3) or when indenting a neutrophil in the back while it phagocytes a bead at its other extremity (10, 14).
27. Custom metal plates and right-angle bracket (#6 in Fig. 1a) to support the piezoelectric stage.

28. Closed-loop piezoelectric stage connected by USB cables to the computer. Matlab drivers for this piezoelectric stages are available on the manufacturer website.
29. Second right-angle bracket to support a rod-holding clamp (#4 in Fig. 1a).
30. Rod-holding joint with tilt adjustment mechanism and attachment pieces to the manual 3-axis micropositioner (#19 in Fig. 1a).
31. Manual 3-axis micropositioner (#18 in Fig. 1a) placed on top of a rigid stand with platform (#17 in Fig. 1a).
32. Two micropipette holders. One holder (#2 in Fig. 1a) has its tubing connected to the water reservoir and held at a 45° angle on the motorized micromanipulator (#7 in Fig. 1a). The other holder is either coming with the microinjecter (#15 in Fig. 1a) and connected with the flexible micropipette to apply aspiration pressure on the air inside (no need for a water reservoir in that case), or does not need tubing in case a closed microindenter is used. More sophisticated reservoir systems are used by others to apply hydrostatic pressure to the cell (16), but they require more tubing hence more potential troubleshooting. As we only need to apply one value of pressure throughout an experiment, we go for a simpler and robust system with only one reservoir and a micropipette holder connected to it.
33. Straight metal rod or alternatively a piece of piano cord to remove glass debris when a pipette is broken inside the body of the micropipette holder.
34. Micropipette puller.

Water reservoir

35. Vertical manual stage supporting the water reservoir, with coarse and fine translation.

36. Pillar made of an optical rail equipped with a mounting plate, and mounted on the optical table with a vertical mounting plate.

Micropipette manufacturing

37. Microforge to cut pipettes open and to melt their tip. A glass bead of about 0.5 mm is placed on the microforge filament and melts when heated by the current passing through the platinum filament of the microforge.
38. Microforge used to bend pipettes.
39. Microinjector to apply negative pressure when using an open flexible micropipette.
40. Short micropipette holder.
41. Commercial force probe to calibrate the bending stiffness of reference microindenters. To facilitate the placement of the head of the probe in front of a low (4, 10 or 20x) magnification objective, you can place the head of the probe on a miniature manual stage which can then be placed on the stage of the inverted microscope. It might be helpful to connect the output voltage of the probe to an oscilloscope to visualize the signal and make sure it is stable over time (see Note 4).

3. Methods

Glass micropipettes can break so be mindful when manipulating them, and take all required cautions when manipulating cells.

3.1 Fabrication of cell-holding micropipettes

1. Pull a borosilicate glass capillary with the micropipette puller with the appropriate program for stiff pipettes (on our micropipette puller: P=500, Heat=474(=ramp+4), Pull=50, Vel. = 140, time = 100).
2. Cut the extremity of the pulled capillary to the desired diameter using the microforge (Fig. 2a). Measure the inner diameter using calibrated graduations in the microforge ocular. Demonstrations videos can be found on our web page (https://cellmechanics.jimdofree.com/videos/) and on Narishige's website (http://products.narishige-group.com/group1/MF-900/injection/english.html).
3. Bend the micropipette at a 45° angle so that when held by the 45°-angled micropipette holder, the tip lies parallel to the bottom of the dish. To do so, place the micropipette at 20-100 µm away from the microforge filament, where the pipette is 50-µm thick. Heat the filament enough (~80% level) for a short period of time (about one second) so the filament start bending. Repeat this heating step until the desired 45°-angle is reached. During the process, adjust the pipette location if it becomes too close to the heating wire. Demonstration videos can be found on our web page (https://cellmechanics.jimdofree.com/videos/) and on Narishige's website (http://products.narishige-group.com/group1/MF-900/injection/english.html). Beware, if you bend the capillary where it is only 20-µm thick or less, instead of bending downwards it will bend upwards. Measure the bending angle using the angular grid in the microforge ocular.

3.2 Fabrication of flexible micropipettes and microindenters

1. Pull a borosilicate glass capillary with the micropipette puller; use the appropriate program for flexible micropipettes (on a our micropipette puller: P= 400, Heat= 517 (= ramp+47), Pull= 50, Vel.= 140, time= 89).
2. Cut the taper of the pulled capillary at a tip diameter of typically 1-2 µm. Heat the tip for a few seconds while it is a few microns from the microforge glass bead to make the borders of the micropipette's tip smooth. This will help forming a tight seal when aspirating a microbead.
3. To know if you need to further shorten the micropipette, roughly estimate the bending stiffness of this micropipette by pressing its tip against the tip of a microindenter of known stiffness (see 3.4). If the stiffness is still too low (<0.1 nN/µm), bring back the freshly cut micropipette, shorten if by typically 50 µm. Repeat these steps until the stiffness is of the desired value, typically 0.2-0.5 nN/µm (see Note 5).
4. Once this is achieved, if you aim for an open flexible micropipette, bend it at a 45° angle where it is 50-µm thick on the micro-forge. If you aim for a microindenter, first plunge the pipette tip in the liquid droplet inside the micro-forge and remove is quickly, the viscous liquid will be carried out on the pipette. Then heat this droplet at distance (~10µm) to make the droplet of molten glass round up. Stop the current in the filament as soon as you reach the desired shape (Fig. 2b). Adapt the velocity when withdrawing the pipette from the molten glass to get different sized droplet (the faster the retraction, the larger the droplet). For droplets of only ~5 µm in diameter, you may just melt the tip at

distance and wait the droplet to become round enough. Measure the diameter of the indenter using the graduations in the microforge ocular. Usually we aim for indenter tips that are 5 to 10 μ m in diameter.

5. Determine more accurately the microindenter tip diameter using a 40x or 100× objective.

3.3 Calibrate a reference microindenter using a commercial probe.

1. Place the commercial probe on the stage of a microscope. One can also perform this calibration under the monitoring of a simple USB camera, as the deflection of the microindenter is done by measuring the position of its base through a manual translation stage (with few microns accuracy), not based on the camera image.
2. Place the microindenter on the manual micromanipulator so that is can be pressed against the tip of the probe (Fig. 2c).
3. Move the base of the microindenter by a known distance imposed by the manual translation stage, check that the analog output signal of the probe is stable by visualizing it on an oscilloscope. Check visually through the camera image that there is not slippage of the microindenter tip. The probe will not deflect, so the microindenter deflection equals the position of its base minus the position when contact with the probe is established (as detected by a deflection of the signal from its baseline value).
4. Establish a voltage-deflection curve, which should be linear. Verify that there is no hysteresis. Perform a linear regression to determine its slope. Divide the V/μm slope by the volts-to-newton conversion factor provided by the probe manufacturer to obtain the bending stiffness of the microindenter, in N/m. Aim for a microindenter soft enough so

that it will not be too stiff when compared to the stiffness of microindenters used to indent cells. However, it should be stiff enough to lead to an accurate calibration with the commercial probe. Aim for typically 20 nN/µm.

5. This 20 nN/µm stiffness is too high to compare directly with a 0.5 nN/µm microindenter, so using this reference indenter of so-called generation 1, calibrate another indenter, of generation 2, with a stiffness of typically 2 nN/µm. To do so, use the technique described in 3.4. Although this will propagate an experimental error, this propagated error is typically of less than 5%. This generation 2-microindenter will be the one to calibrate your microindenters used for cell indentation.
6. Keep carefully your reference indenters in a large closed Petri dish to avoid dust and shocks.

3.4 Calibration of the bending stiffness

To measure the bending stiffness of a newly pulled microindenter or flexible micropipette, we press its tip against the tip of a reference microindenter of known bending stiffness. It is important that this reference microindenter has a glass bead at its tip because this will ensure that is it not broken (a broken micropipette might look a lot like an intact micropipette). The base of the microindenter of unknown stiffness is translated to press its tip against the tip of the reference microindenter (Fig. 2d). The forces exerted by each cantilever in quasi-static conditions balance each other, so that $k_1 d_1 = k_2 d_2$, where k_1 and k_2 are the bending stiffness of the reference and new microindenter, respectively, and d_1 and d_2 their respective deflection. By plotting d_2 *vs* d_1, one gets a linear curve (Fig. 2d) of slope k_1/k_2, from which k_2 is deduced based on the already known

value of k_1. It is immediate that any error on k_1 is propagated to k_2. In practice we dedicate a small setup to calibration. It has a piezoelectric stage which performs an oscillatory translation of the base of the microindenter of unknown stiffness. For calibration we use a 40x air objective. No Petri dish is needed at this step. Beware that in air, micropipette will stick quite well due to electrostatic interactions. One can use the same setup as for experiments, using a dedicated calibration is only a matter of user-friendliness. Other groups have developed interesting alternatives to calibrate pipette stiffness such as using a hanging droplet (8). It is also possible to use small weights such as pieces of metallic wires (17, 18) or pieces of paper (3) to a calibrated reference fiber, but this procedure might be more difficult in practice.

3.5 Automated detection of the force and indentation, and feedback loop

The position of the tip of the microindenter is measured each time the camera acquires a new image (at a rate of typically 400 Hz, see Note 6). In the configuration described in Figure 1, the cell is pushed against the indenter, so that indenter deflection is the difference between the tip's updated position and its position under no force measured at the start of the experiment (Fig. 3; see Note 7). The force applied to the cell is the product of the microindenter deflection and the microindenter bending stiffness *k*. An algorithm implemented in Matlab runs a feedback loop (see Note 8) that controls the piezoelectric stage position based on the analysis of each new image. The experiment is decomposed in several phases, each one defining a different behavior of the feedback loop. We start an experiment with the cell facing the microindenter's tip, a few microns away from it (Fig. 1b-d). During a first phase, the cell is moved at constant velocity, typically 0.25-0.5 µm/s, toward the microindenter. Once cell-indenter contact is made (which is

detected upon reaching a microindenter deflection threshold of typically 0.1 µm), the compressive force applied to the cell increases, until a force threshold is reached (typically 0.1-0.5 nN on leukocytes, up to few nN on stiffer cells such as endothelial cells). The algorithm then automatically switches to a second phase, during which various options are possible: applying an oscillatory force around an average value at a constant frequency (typically 1 Hz) (10, 14), keeping the force constant and recording the evolution of indentation over time (creep experiment), or keeping the indentation constant and measuring the decrease in force over time (force relaxation experiment). Once this phase is over (after a preset duration is over), the cell is retracted at constant velocity.

3.6 Microindentation of non-adherent cells

1. Prepare 10 mL of cell buffer and a Petri dish. Put a droplet of immersion oil on the objective and place the dish on the 100x oil objective. Add 3 mL of medium at room temperature (see Note 9) in the dish.
2. Fill the water reservoir with ultra-pure water. Position the 4-way stopcock to fill the auxiliary micropipette connected to the reservoir. Make sure no bubble is trapped in the 4-way stopcock.
3. Switch the 4-way stopcock so the auxiliary pipette filled with water is directly connected to the tubing of the micropipette holder, and fill the tubing with water.
4. Connect a syringe to a blunt fill needle with a piece of rubber joint at its tip. Connect this auxiliary air syringe to the back of a pre-forged stiff micropipette and dip its tip in a tube of DPBS while making sure not to touch the tube walls (use a 15- or 50mL tube, and you

can reuse it for several days, at room temp in pure DPBS contamination is limited). Exert aspiration pressure with the syringe (see Note 10). Complete the filling of the micropipette through its back using a syringe filled with water and connected to a long capillary. You should be able to avoid any bubble, but if you trap one (which will be obvious by eye inspection), gently flick the micropipette with the nail, several times. You will see the bubble deform and eventually detach from the inner wall of the micropipette. Use again the capillary to make sure the bubble doesn't stay trapped at the meniscus at the back of the capillary.

5. Connect this liquid-filled pipette with the micropipette holder. Hold the latter below the water level in the reservoir so drops start flowing. Make the meniscus at the back of the pipette coalesce with a droplet dripping from the capillary tip in order to avoid trapping any bubble. Bubbles will forbid any efficient aspiration and will create hysteresis when changing the height of the water reservoir (see Note 11).
6. Place the micropipette tip on the microscope and center it in the field of view. We usually use the camera with stretched histogram to do so. See Note 12 for finding your micropipette on the microscope. Place the tip typically 30 µm above the bottom (on our microscope, a full revolution of the fine z knob corresponds to 100 µm).
7. Set Köhler illumination, which is important get the best out of the optical setting.
8. The difference in height Δh between the water level in the reservoir and the water level in the dish sets an hydrostatic pressure difference, $\Delta P = \rho g \Delta h$, where ρ is the volume mass of the water in the reservoir and tubbing and of the buffer in the dish (both being approximated as equal to 1000 kg/m^3), g is the acceleration of earth gravity field on earth surface ($g \approx 9.8\ m/s^2$). As a result, 1 mm of water difference represents 9.8 Pa of pressure

difference. Put an aspiration corresponding to $\Delta h \approx 5$ mm. This will let the micropipette aspirate some medium and let the serum present in the medium coat the pipette walls. This will minimize adhesion of cells to the surface of the pipette (see Note 2).

9. Place your microindenter (see Note 13). Place the tip of the indenter at about 30 µm above the bottom of the dish (see Note 14).
10. Bring the cells, in our case no need to concentrate them (they are at 0.5-1.0x10^6/mL), inject 50-100 µL of cell solution (see Note 15). Inject at the bottom of the chamber, in the "North" half of the dish (higher values on the y axis following axis convention shown in Figure 1a). The "South" part is less accessible given the angle of the indenter (Fig. 1a) that will hit the border of the Petri dish if you too far towards the South. Gently press the tip of the cone on the bottom of the dish, then gently expulse cell solution, so that cells are not be too diluted in the whole dish (see Note 16). Wait a couple of minutes for cells to sediment, then find the zone where cells are more concentrated.
11. Set the zero of aspiration pressure by changing the height of the reservoir. It is very helpful to know already quite well (within a millimeter) where the zero should be (put a mark on you reservoir). Adjust the reservoir height using the fine translation (#10 in Fig. 1a) so that the micropipette tip neither aspirates nor blows. To probe if the pipette is aspirating of blowing, you can use a bead that is not stuck to the bottom (or unstick it by scratching the pipette tip against it), or a cell but being careful not to aspirate is too much so that its membrane stays intact. You can also use a cell debris. Once zero is known, set the aspiration level for the experiment, Δh is typically 3-5 mm.
12. Aspirate a cell, and place it in front of the tip of the indenter (Fig. 1b-d).
13. Prepare in advance the parameters of the experiment (see Note 17).

14. Add all necessary remarks in a note book: unusual aspect of cell, cell-bead misalignment etc.
15. You may need to slightly adjust the relative cell-bead position in-between experiments.
16. Once a cell has been probed, to avoid re-testing it by mistake, move the microscope stage (see Note 18) to go to extreme North positon in the dish (by moving microscope stage towards increasing values of y). Gently nail-flick the cell holding pipette to expulse cell, and move back to a zone where there are many cells to run another experiment (see Note 19).
17. Scrutinize the aspects of cells. With no control of pH, do not expect to run experiments typically more than 2 hours. After this time lapse: take out the pipette and the indenter (fix them in a safe place next to the microscope), then change the dish. When taking the dish out, clean the oil on the objective (kimwipes or equivalent are fine) and put a new oil droplet, experience shows that this minimizes the appearance of bubbles in the oil.

3.7 Microindentation of adherent cells

We have developed a strategy to use profile microindentation on adherent cells by culturing them on large (200 µm-) dextran beads, which allows observing cell deformation upon indentation (Fig. 1d). During cell indentation, the dextran is held in place using a micropipette with a tip of 10-50 µm (3)(see Note 20).

3.8 Microindentation using an activating microbead

The techniques described above use an indenting surface whose role is only to press on the cell to deform it. However, one might want to follow mechanical changes induced by the engagement of receptors at the surface of the cell. To do so, instead of a microindenter, one can use a micropipette aspirating a microbead that is coated with molecules of interest, e.g. antibodies targeting some specific receptors on the cells. We have used this strategy to follow mechanical changes in leukocytes during their activation following the engagement of their receptors. In that case, the indenter becomes an adhesive surface, and the bead cannot be detached after the first contact. One can apply force modulation once this first contact was made. This allows extracting the initial Young's modulus of the cell, and the evolution of the complex stiffness of the cell-bead contact over time (10, 14).

3.9 End of experiments

1. Remove the micropipette and the microindenter (see Note 21).
2. Throw out the Petri dish in a trash suited for the biological material you are working with.
3. Remove the oil on the oil objective.
4. Empty the water reservoir using the auxiliary syringe, then rinse the reservoir with ethanol and flow it in the tubing and in the micropipette holder.
5. Clean the microscope stage with ethanol.
6. Save all data if not done already, and turn everything off (camera, computer, microscope lamp etc).

3.10 Data and statistical analysis

After acquisition of raw data (Fig. 4), we analyze them using a custom Python code. One task is to determine the contact point, when force starts increasing, via post-processing of raw data (several strategies exist, see e.g. ref. (19)). Finite thickness correction can be used when calculating the Young's modulus (20).

4. Notes

1. We use thin-walled glass capillaries to make both stiff and flexible micropipettes, but thick-wall could also be used after adapting the puller settings. Capillaries do not need to have a filament. A filament might actually become a problem for the tight seal between the flexible micropipette and a bead.
2. Although some groups performing micropipette aspiration use micropipette passivation (22), we always work with serum present in the medium (usually 10% fetal calf serum) and rely on the albumin present in the serum to passivate glass surfaces and make them non-adhesive. Yet, cells might become slightly adherent through discrete spots/tubes, and it might not be immediate to expulse a cell from the cell-holding pipette. In that case nail-flicking the pipette holder will usually create a vibration strong enough to detach the cell. The same issue might happen because the bead held by the flexible micropipette can be a bit sticky. In that case a stronger nail flicking might be needed, but beware that this might

propagate to the surrounding of the flexible micropipette and expulse the cell held aspirated by the other micropipette.

3. Avoiding vibrations is important for signal quality, even more so when using soft microindenters and high-magnification objective. Avoid any tension in wires, e.g. in the possibly heavy wires linking the camera to the computer. Avoid as much as possible placing objects with fans on the insulating table. It might be useful to enclose the whole setup inside an acoustic insulation case, although this will make the access to the setup less user-friendly – we do not use such case. Avoid the vicinity of air conditioning and open window in the room.
4. What we describe here is a setup that has benefited from about 10 year of accumulation of hardware. One can start with a less comfortable but less expensive version, for instance by using only manual micromanipulators, no commercial force probe, a simpler water reservoir with only a coarse translation, and a less expensive microscope stage (even a custom simple microscope stage can be applicable).
5. Adjust the stiffness of the cantilever by adjusting the puller settings, cutting the micropipette longer or shorter. See the "pipette cookbook" on Sutter Instrument website for many useful tips (https://www.sutter.com/MICROPIPETTE/cookbook.html).
6. Fast camera-to-computer transfer rate ensures an optimized acquisition rate. Provided the exposure time is not the limiting step (we expose 1 to 2 milliseconds only), this rate depends on the camera and connectivity (USB3 or Camera Link interface card for instance), and also importantly on the size of the region of interest (ROI) selected in the Matlab code via Micro-Manager. For a ROI of 600 x 400 pixels, we typically get a rate of acquisition of 400 Hz. Note that not every image is stored, which would dramatically

decrease the acquisition rate: only a line is analyzed to determine the position of the indenter on the fly through a cross-correlation operation (Fig. 3). This raw data can then be smoothed during post-processing using for instance a sliding-window average. We keep a full image every 1 or 2 s to monitor the morphology of the cell.

7. When designing over which micropipette holder you should place the piezoelectric stage, two options are possible: either pushing the cell against the indenter, or pushing the indenter against the cell. Although this might seem equivalent, there will be differences e.g. the hydrodynamic drag will be higher on the flexible micropipette if it is the one being translated by the piezoelectric stage. In our later evolution of the setup presented here, we push the cell against the microindenter. If the cell moves, the deflection of the indenter will simply be the displacement of its tip relative to its initial resting position. The cell indentation will be obtained by measuring the difference between the displacement of the piezo stage and the position of indenter's tip. On the contrary, if the indenter is the one being pushed against the cells, the deflection of the indenter will be obtained by measuring the difference between the position of the piezoelectric stage and the position of the indenter's tip. In the latter case, the indentation of the cell will simply be the position of the indenter's tip relative to its position when contacting the cell.
8. It is possible to implement a live feedback loop to apply an arbitrary controlled force to the cell. The same principles apply to design a feedback loop on cell indentation. We introduce an error signal that is the difference between the actual microindenter deflection and the desired microindenter deflection (the latter being the ratio between the target force and the microindenter stiffness). At each time step, the new piezoelectric position is set to its actual position plus a quantity that is the error signal multiplied with a constant

proportional coefficient. This is a very simple implementation that has been proven to work satisfactorily in our setup. However, much more sophisticated feedback algorithms can be implemented (including a PID controller where a term proportional to the integral and the derivative of the error signal are added) (23), at the expense of more complexity of the algorithms and potential difficulties to tune the additional feedback parameters.

9. Working at 37°C is a challenge using the microindentation technique described here. The dish can be heated using a heating plate, eventually complemented with an objective heater. However, because we work in a relative large volume of 3 mL in an open dish, this type of heating is quite inefficient, and will lead to strong temperature gradients inside the dish. To work at 37°C, we would advise to adapt the setup to work in a smaller volume, and eventually to work on a way to circulate medium at 37°C (but stopping circulation during experiments). Another option is to enclose the whole setup in a temperature-controlled chamber, but beware that the electronics (piezo stage, micromanipulator) might get damaged over time, especially if you also control humidity. Such an enclosure might not prevent from the presence of strong temperature gradients, and air flow within the chamber might disturb measurements. Using large metallic pillars as we do is problematic, because of the large dilation and thermal that can occur in the pillar. If the tubing of the micropipette is also at 37C, bubbles will form much more often than at room temperature, which might block cell aspiration and require reinstalling pipettes regularly. Consider sonicating the medium to expulse gas before experiment in that case. We have shown in the past that leukocyte dynamics are faster when close to 37°C although qualitatively they behave the same (10). Given these considerations, we generally work at room temperature.

10. Hydraulic resistance varies with a power 4 of the pipette tip diameter, so filling the tip of micropipette is much harder when it is 2 µm than 3 µm in diameter. When using tips of diameter smaller than 2 µm, be patient. Tips of 1 µm and less are in practice not possible to fill within a reasonable time and in that case using capillaries with filaments will be required.
11. If you see that passing to a positive pressure by raising the water reservoir does not stop aspiration, this is mostly due to a bubble present inside the micropipette holder or its tubbing. If you can live with inaccurate aspiration (some experiments allow that) you can make sure the pipette aspirates using a very large height difference of the water reservoir. However, the best is usually to take out pipette, unplug it, eventually cut its back few millimeters with a diamond (a cheap synthetic diamond will be enough), and replace it, or even use a new micropipette.
12. Micropipette placement can be done using only a 100x oil objective, without the need to switch to an air objective of lower magnification. However, this asks for a bit of training. The key to find and center micropipettes is to close the condenser aperture diaphragm (#21 in Fig.1a), eventually to increase exposure time to about 50 ms to optimize contrast, and to use the image on screen with histogram stretching so as to see the "shadow" of the pipette passing well-above the focus plane (up to hundreds of microns) when moving it along the *x*-axis past the center of the objective (axis convention shown in Fig. 1a) with the pipette being well passed the center towards positive y values. This will ensure that the part of the micropipette shaft that crosses the field of view when moving it along the *x*-axis is thick, hence more easily seen. Once the tip was found and centered in the field of view, the micropipette has to be lowered in order to find where the bottom of the Petri

dish exactly is. When lowering the pipette, if it hits the bottom, it will start moving in the x-y plane because it is getting bent. One advantage of using pipettes whose tip is parallel to the bottom and that are relatively flexible is that pipettes will tolerate bending in contact with the bottom before breaking. Alternatively, if one prefers switching objectives, beware of bubbles that can form when switching back to the oil objective. Do not forget reopening the condenser aperture diaphragm when ready for running the experiment, with proper Köhler illumination setting.

13. The microindenter is more valuable than the pipette so place the micropipette first, it will minimize the risk of breaking the microindenter while searching for the bottom of the dish.
14. Working about 30 µm above the dish is a trade-off between a good image quality (the better the closer from the bottom of the dish) and not having the image disturbed by cells present at the bottom of the dish. Make sure the microindenter shaft does not touch another cell outside of the field of view.
15. Some groups cut 1-mL pipette cones to minimize shear, but in our hands, injecting with unmodified 200-µL cone is not a problem.
16. An alternative to inject cells is the falling drop technique. Inertia will mix the droplet, but it will disperse and dilute cells. Cells might take a longer time to sediment, and you might need to add more cells using this technique.
17. The most important parameters to be set in a code are: data log (date, cell#, file path, list of parameters used); frequency for force modulation experiments; piezo velocity for approach/retraction phase; number of approach-retraction cycles; duration at contact once the maximal force threshold is reached (can be 0 to several minutes); indenter bending

stiffness; detection threshold to roughly determine is cell-microindenter contact was made (~0.1 µm); maximal force (0.1-0.5 nN); average force and amplitude when using force modulation (typically f = 0.2 ± 0.03 nN); exposure time; proportional coefficient for feedback loop; pixel size corresponding to the objective (in µm); dimension of the region of interest (w*h in pixels).

18. We avoid motorized x-y stages on the microscope. In our hands a manual x-y translation is more reactive (and cheaper) than a motorize one. An experienced user can have a surprising micron-size accuracy with his/her bare hands on the x-y manual translation knobs when centering the stage on a chosen cell at the bottom of the dish.
19. The expected data throughput with the technique will be relatively low, but will depend on the type of experiment. For a single indentation of a cell to measure its effective Young's modulus, one can go down to 2 minutes per cell. But experiments can extend up to 30 minutes per cell. Beyond this duration, drift of the micropipettes might become too large (especially if working above room temperature).
20. Several extensions can be added to the setup, for instance a third micropipette used to flow a solution of interest on the cell being indented (3). Fluorescence imaging can be added and snapshots under fluorescence excitation can be acquired automatically in-between indentations by modifying the Matlab code.
21. You can try re-using flexible pipettes, but beware that upon drying they might get clogged and contaminated. We usually use one flexible pipette for the whole day. We usually re-use microindenters several times provided they do not get dirty due to adhered cells or cell debris.

5. References

1. Guck, J. 2019. Some thoughts on the future of cell mechanics. Biophys. Rev. 11: 667–670.

2. Guillou, L., R. Sheybani, A.E. Jensen, D. Di Carlo, T.S. Caffery, C.B. Thomas, A.M. Shah, H.T.K. Tse, and H.R. O'Nea. 2021. Development and validation of a cellular host response test as an early diagnostic for sepsis. PLoS One. 16: 1–17.

3. Guillou, L., A. Babataheri, P.-H. Puech, A.I. Barakat, and J. Husson. 2016. Dynamic monitoring of cell mechanical properties using profile microindentation. Sci. Rep. 6: 21529.

4. Sawicka, A., A. Babataheri, S. Dogniaux, A.I. Barakat, D. Gonzalez-Rodriguez, C. Hivroz, and J. Husson. 2017. Micropipette Force Probe to quantify single-cell force generation: application to T cell activation. Mol. Biol. Cell. 28: mbc.E17-06-0385.

5. Colbert, M.-J.J., A.N. Raegen, C. Fradin, and K. Dalnoki-Veress. 2009. Adhesion and membrane tension of single vesicles and living cells using a micropipette-based technique. Eur. Phys. J. E. Soft Matter. 30: 117–21.

6. Colbert, M.-J.J., F. Brochard-Wyart, C. Fradin, and K. Dalnoki-Veress. 2010. Squeezing and detachment of living cells. Biophys. J. 99: 3555–62.

7. Backholm, M., W.S. Ryu, and K. Dalnoki-Veress. 2013. Viscoelastic properties of the nematode Caenorhabditis elegans, a self-similar, shear-thinning worm. Proc. Natl. Acad. Sci. 110: 4528–4533.

8. Backholm, M., and O. Bäumchen. 2019. Micropipette force sensors for in vivo force measurements on single cells and multicellular microorganisms. Nat. Protoc. 14: 594–615.

9. Francis, G.W., L.R. Fisher, R.A. Gamble, and D. Gingell. 1987. Direct measurement of cell detachment force on single cells using a new electromechanical method. J. Cell Sci. 87 (Pt 4): 519–23.

10. Zak, A., S.V. Merino-Cortés, A. Sadoun, F. Mustapha, A. Babataheri, S. Dogniaux, S. Dupré-Crochet, E. Hudik, H.-T. He, A.I. Barakat, Y.R. Carrasco, Y. Hamon, P.-H. Puech, C. Hivroz, O. Nüsse, and J. Husson. 2021. Rapid viscoelastic changes are a hallmark of early leukocyte activation. Biophys. J. 120: 1692–1704.

11. Guillou, L., A. Babataheri, M. Saitakis, A. Bohineust, S. Dogniaux, C. Hivroz, A.I. Barakat, and J. Husson. 2016. T-lymphocyte passive deformation is controlled by unfolding of membrane surface reservoirs. Mol. Biol. Cell. 27: 3574–3582.

12. Samassa, F., M.L. Ferrari, J. Husson, A. Mikhailova, Z. Porat, F. Sidaner, K. Brunner, T. Teo, E. Frigimelica, J. Tinevez, P.J. Sansonetti, M. Thoulouze, and A. Phalipon. 2020. Shigella impairs human T lymphocyte responsiveness by hijacking actin cytoskeleton dynamics and T cell receptor vesicular trafficking. Cell. Microbiol. 22: 1–15.

13. Merino-Cortés, S. V., S.R. Gardeta, S. Roman-Garcia, A. Martínez-Riaño, J. Pineau, R. Liebana, I. Merida, A.-M.L. Dumenil, P. Pierobon, J. Husson, B. Alarcon, and Y.R. Carrasco. 2020. Diacylglycerol kinase ζ promotes actin cytoskeleton remodeling and mechanical forces at the B cell immune synapse. Sci. Signal. 13: eaaw8214.

14. Zak, A., S. Dupré-Crochet, E. Hudik, A. Babataheri, A.I.A.I. Barakat, O. Nüsse, and J. Husson. 2022. Distinct timing of neutrophil spreading and stiffening during phagocytosis. Biophys. J. : 1–14.

15. Edelstein, A.D., M. a Tsuchida, N. Amodaj, H. Pinkard, R.D. Vale, and N. Stuurman. 2014. Advanced methods of microscope control using μManager software. J. Biol. Methods. 1: 10.

16. Lam, J., M. Herant, M. Dembo, and V. Heinrich. 2009. Baseline mechanical characterization of J774 macrophages. Biophys. J. 96: 248–54.

17. Shimamoto, Y., and T.M. Kapoor. 2012. Microneedle-based analysis of the micromechanics of the metaphase spindle assembled in Xenopus laevis egg extracts. Nat. Protoc. 7: 959–969.

18. Desprat, N., A. Guiroy, and A. Asnacios. 2006. Microplates-based rheometer for a single living cell. Rev. Sci. Instrum. 77: 055111.

19. Lin, D.C., E.K. Dimitriadis, and F. Horkay. 2007. Robust strategies for automated AFM force curve analysis--I. Non-adhesive indentation of soft, inhomogeneous materials. J. Biomech. Eng. 129: 430–40.

20. Dimitriadis, E.K., F. Horkay, J. Maresca, B. Kachar, and R.S. Chadwick. 2002. Determination of elastic moduli of thin layers of soft material using the atomic force microscope. Biophys. J. 82: 2798–810.

21. Hertz, H. 1882. Ueber die Berührung fester elastischer Körper. J. für die reine und Angew. Math. 92: 156–171.

22. Guevorkian, K., and J.-L. Maître. 2017. Micropipette aspiration. In: Methods in Cell Biology. Elsevier Ltd. pp. 187–201.

23. Bechhoefer, J. 2005. Feedback for physicists: A tutorial essay on control. Rev. Mod. Phys. 77: 783–836.

Figure Legends

Fig. 1 Experimental setup for profile microindentation. **(a)** Schematic of the main components of the setup: **1** Glass-bottom Petri dish with buffer, cells, and eventually microbeads; **2** micropipette holder (for the cell-holding micropipette); **3** micropipette holder (for the microindenter/ flexible micropipette); **4** right-angle bracket and rod-holding clamp; **5** uniaxial piezoelectric stage; **6** right-angle bracket and plates linking the 3-axis motorized micromanipulator and piezoelectric stage; **7** motorized micromanipulator; **8** rigid stand with platform supporting the head of the motorized micromanipulator; **9** pillar and mounting plates; **10** vertical manual stage supporting the water reservoir, with coarse and fine translation; **11** 50-mL plastic syringe used as the body of a water reservoir; **12** auxiliary syringe used to adjust water level and exert strong pressure connected via a 4-way stopcock; **13** x-y stage translation knobs; **14** anti-vibration optical table; **15** microinjecter; **16** camera; **17** rigid stand with platform; **18** three-axis manual translation stage; **19** rod-holding joint with tilt adjustment mechanism, and attachment pieces to the 3-axis manual translation stage; **20** microscope stage; **21** condenser aperture diaphragm; **22** field diaphragm; **23** microscope illumination. The inset shows a schematic view of the micropipette tips (not to scale); **24** cell-holding micropipette; **25** flexible micropipette or microindenter; **26** cell and microindenter/bead aspirated by the flexible micropipette. Part of the microscope body is not shown, including the oculars, the objective, and an eventual fluorescent light source. **(b-d)**: Microscopy image in DIC (b-c) and brightfield illumination (c) of different cells being studied. **(b)** Microscopy image of a leukocyte (human CD4 T lymphocyte) held aspirated by the stiff micropipette (left) and flexible micropipette holding an antibody-coated microbead aspirated

(right). Scale bar: 10 µm. See (4, 11) for similar configuration. **(c)** Microscopy image of a leukocyte (neutrophil-like PLB cell) held aspirated by the stiff micropipette (left) and microindenter on the right. Scale bar: 10 µm. See (10) for similar configuration. **(d)** Endothelial cell grown on a 200-µm dextran bead held by a stiff micropipette on its left extremity, and microindenter (right). Scale bar: 10 µm. See (3) for similar configuration.

Fig. 2. Micropipette fabrication and calibration. **(a)** Once they are pulled, micropipettes are cut using a microforge. The tip of the micropipette is dipped into a drop of molten glass present on the heating filament of the microforge. A sequence of steps (i-iv) is followed to cut the tip at a desired diameter. Left column: microscopy image taken on the microforge (bar: 10 µm). Right column: schematic view (not to scale). Steps (i-iv) are repeated a few times until the desired diameter (typically 3-µm inner diameter) is reached. A demonstration video can be found online (https://cellmechanics.jimdofree.com/videos/). **(b)** The microforge is used to form a glass microbead at the tip of a flexible micropipette. A micropipette is dipped into the drop of molten glass and quickly retracted to carry some molten glass with it. Once a droplet has been deposited at the tip of the micropipette (i-iii), it can be made more spherical by heating it at distance (iv). Steps (i-iv) can be repeated to form a larger bead. Left column: microscopy image taken on the microforge (bar: 10 µm). Right column: schematic view (not to scale). A demonstration video can be found online (https://cellmechanics.jimdofree.com/videos/). **(c)** The measurement of the bending stiffness of a reference microindenter is performed by pressing it against a commercial force probe. The probe and microindenter are schematically represented (not to scale). Inset: the compressive force F exerted by the microindenter on the probe is plotted versus the deflection d

of the microindenter. A linear fit is superimposed. The bending stiffness is the slope of this force-deflection curve. Given the force resolution of the commercial probe, we aim for reference microindenters with a stiffness of about 20 nN/µm. **(d)** Microindenters used routinely are calibrated against a reference microindenter by measuring the ratio of their respective deflection d_1 and d_2 when pressed one against the other. We use a dedicated setup that is similar to the one used during experiments on cells, except that it is equipped with a 40x air objective. The reference microindenter of bending stiffness k_1 is fixed, so the microindenter deflection d_1 equals x_{tip}, where x_{tip} is the position its tip. The base of the microindenter of unknown bending stiffness k_2 is translated by a piezoelectric stage whose position x_{piezo} is recorded. The deflection of this microindenter is $d_2=x_{piezo}-x_{tip}$. **(e)** The translation of the microindenter is slow enough so that inertia can be neglected and forces exerted by the tip of each microindenter equilibrate. As a result, $k_1d_1 = k_2d_2$, so by plotting d_2 against d_1, one gets a line of slope k_1/k_2. As k_1 is known, k_2 can be calculated. Lower right inset: image of indenter tips under the microscope; the scale bar represents 10 µm. Upper left inset: x_{piezo} and x_{tip} are plotted against time.

Fig. 3. Measuring force and cell indentation. **(a)** Schematic view of a stiff micropipette holding a cell (left) and a microindenter (right). The setup is shown before contact (light gray) and upon cell indentation (darker gray) following a translation Δx_{piezo} of the piezoelectric stage along the horizontal x-axis. When the cell is pressed against the tip of the microindenter, the latter bends. Its deflection equals the translation of the tip of the microindenter, $\Delta x_{indenter}$. The force F exerted by the microindenter on the cell is obtained by multiplying the microindenter deflection with the

microindenter bending stiffness, $k_{indenter}$:

$F = k_{indenter}\Delta x_{indenter}$. The indentation of the cell, δ, is the difference between the piezoelectric stage translation and the indenter deflection: $\delta=\Delta x_{piezo}-\Delta x_{indenter}$. To measure the position of the tip of the microindenter, the intensity profile along a line crossing the shaft of the microindenter (x-axis shown on the figure) is analyzed at an acquisition frequency of roughly 400 Hz (see Note 6). An intensity profile acquired at the beginning of an experiment, $I_{template}(x)$, is kept in memory. It is then used as a template that is compared at each time step with the actualized intensity profile, $I_{live}(x)$. The comparison is done by calculating of a cross-correlation shown in b. **(b)** The cross-correlation $C(s)$ of $I_{template}(x)$ and $I_{live}(x)$ is $C(s) = \int (I_{live}(x) - \langle I_{live}\rangle)\big(I_{template}(x-s) - \langle I_{template}\rangle\big)dx$, where s is the shift of $I_{template}(x)$ relative to the live profile $I_{live}(x)$, and brackets represent an average over x. Before cross-correlating them, the average value of I_{live} and $I_{template}$ is subtracted. A typical correlation function is shown on the graph. It presents a maximum at a shift that corresponds to the location of the microindenter tip relative to its position when the template was acquired. The shift takes integer values corresponding to an integer number of pixels. However, by performing a parabolic fit over typically 10 pixels (in red on the graph) around the maximum of the cross-correlation function, the position of the microindenter tip is measured with sub-pixel accuracy. We obtain an accuracy of about 20 nm for a pixel representing 59 nm in the specimen plane using a 100x magnification objective.

Figure 4. Time traces and force-indentation curve. **(a)** Force (red), indentation (blue), and piezoelectric stage translation (x_{piezo}, gray) during the indentation of a T lymphocyte (see an example in Fig. 1b). A first compression phase is performed by translating the piezoelectric stage at constant velocity (dx_{piezo}/dt = 0.25 µm/s) until a preset force threshold is reached, after which

an oscillatory force is applied through the use of a live force feedback loop. After a preset duration is over under oscillatory force, the piezoelectric stage is withdrawn at constant velocity (here again 0.25 µm/s). The inset shows a closer view on the force and indentation signals, with sliding window-averaged values superimposed to raw data acquired at roughly 400Hz. **(b)** Force-indentation curve (red) during the initial compressive phase. Data are fitted with the Hertz model $F = \frac{4}{3}\frac{E}{1-\nu^2}\sqrt{R_{eff}}\delta^{3}/_{2}$ (3, 21) (blue curve), where E is the effective stiffness, ν is the Poisson's ratio taken as 0.5 (see suppl. Mat. in (3)), δ is the indentation of the cell, and R_{eff} an effective radius defined by $1/R_{eff} = 1/R_{indenter} + 1/R_{cell}$, where $R_{indenter}$ is the radius of the microindenter tip or micropipette bead, and R_{cell} is the cell radius.

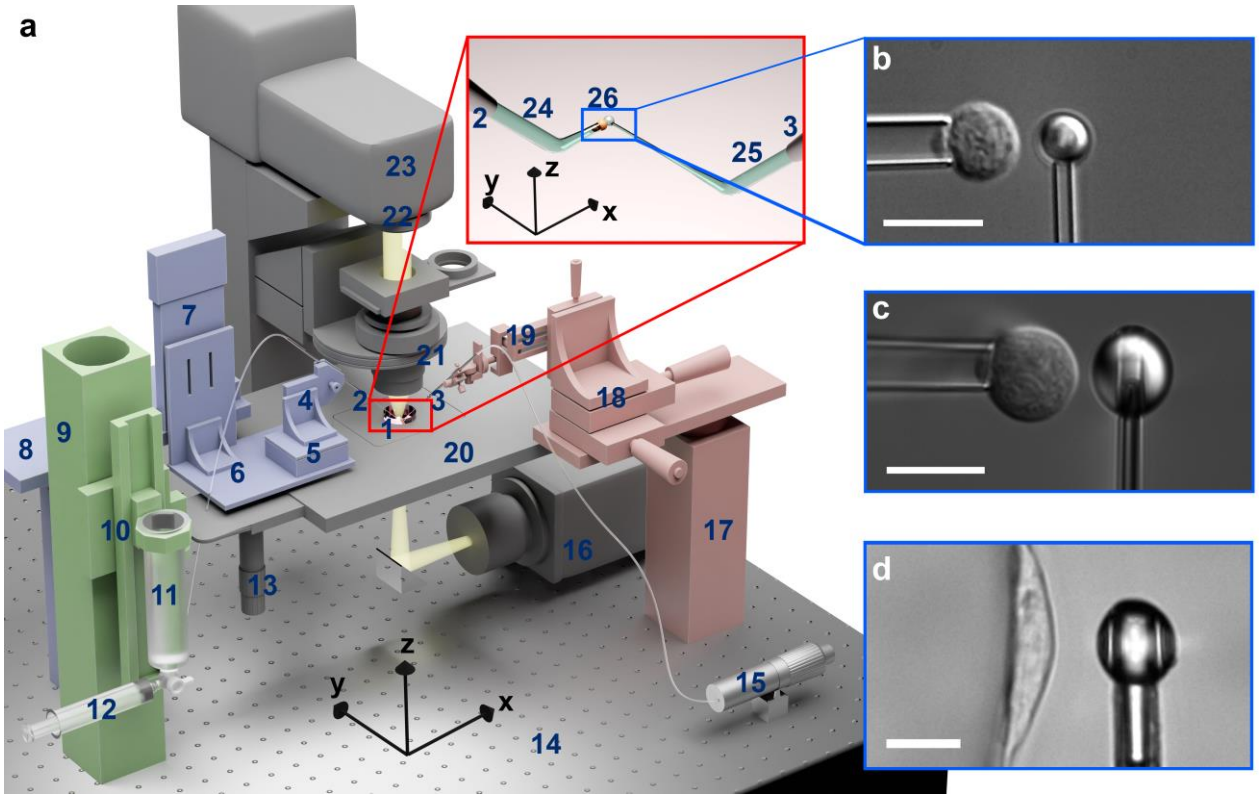
a
b
c
d
1
2
3
4
5
6
7
8
9
10
11
12
13
14
15
16
17
18
19
20
21
22
23
24
25
26
x
y
z

Figure 1

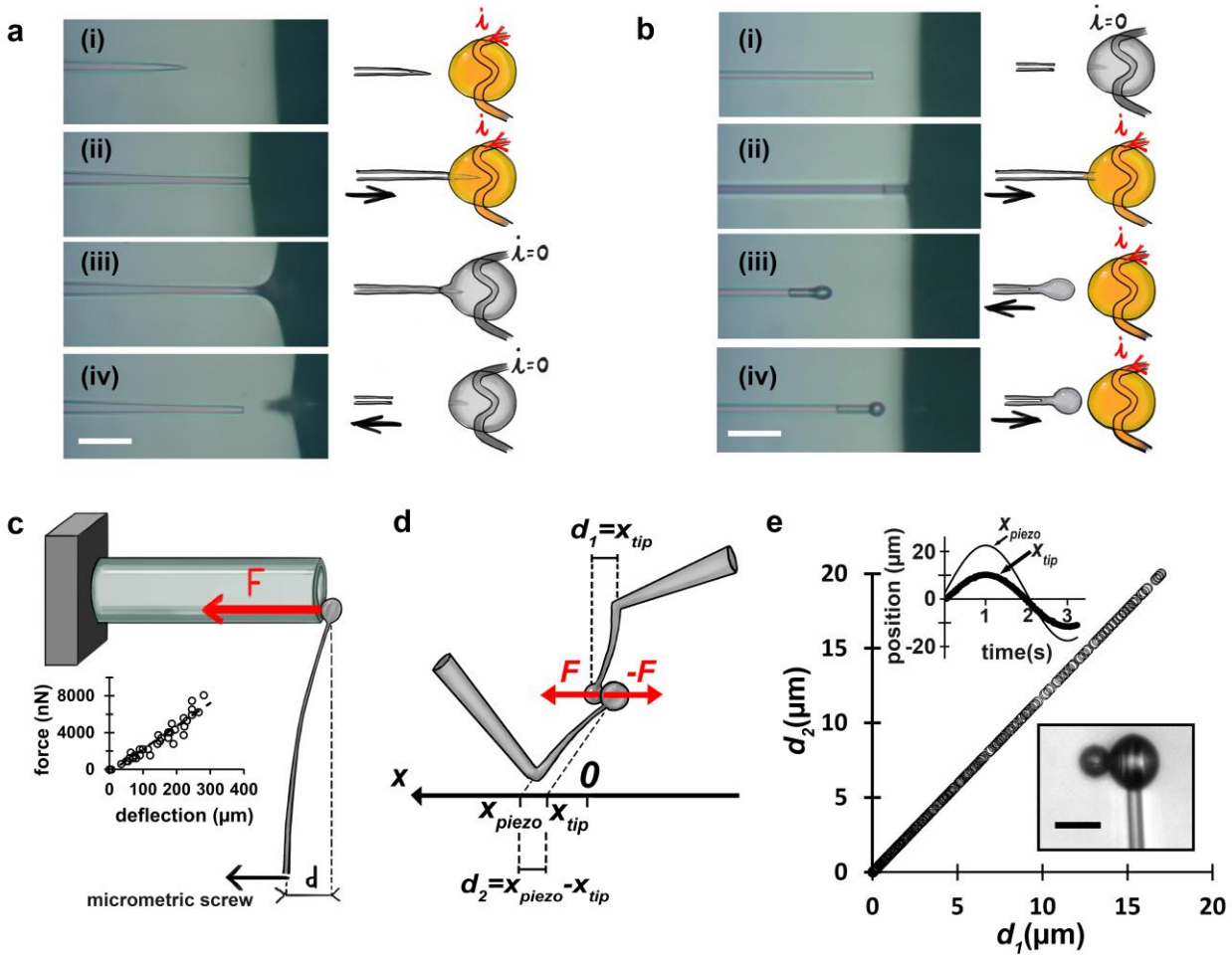
a
(i)
(ii)
(iii)
(iv)
b
(i)
(ii)
(iii)
(iv)
c
F
force (nN)
8000
4000
0
0 100 200 300 400
deflection (μm)
micrometric screw
d
d
d1=xtip
F
-F
x
0
xpiezo
xtip
d2=xpiezo-xtip
e
xpiezo
xtip
position (μm)
20
0
-20
1
2
3
time(s)
d2(μm)
20
15
10
5
0
0
5
10
15
20
d1(μm)

Figure 2

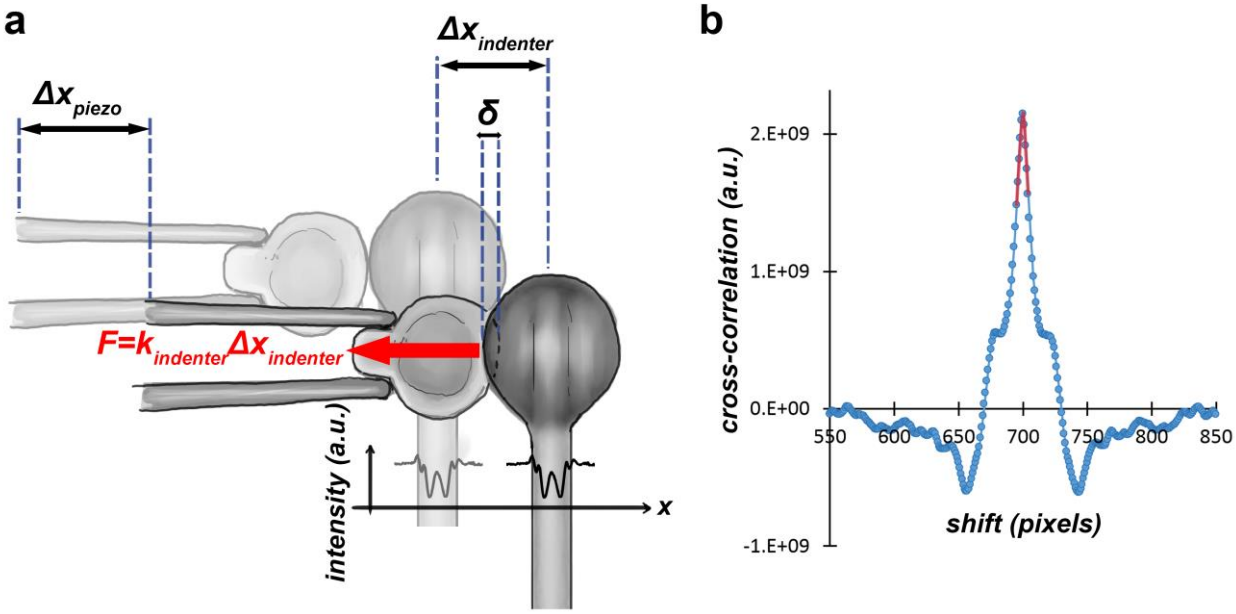
a
Δx indenter
Δx piezo
δ
F=k indenter Δx indenter
intensity (a.u.)
x
b
cross-correlation (a.u.)
2.E+09
1.E+09
0.E+00
-1.E+09
550
600
650
700
750
800
850
shift (pixels)

Figure 3

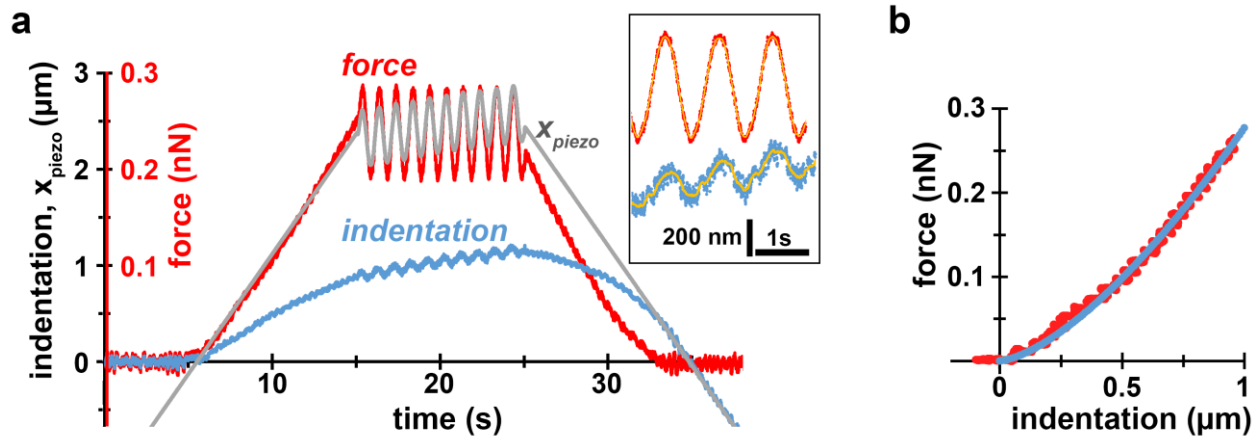
a
b
force
indentation
x_{piezo}
indentation, x_{piezo} (µm)
force (nN)
time (s)
200 nm
1s
indentation (µm)

Figure 4